

EFFECT OF THICKNESS AND ON EFFICIENCY OF IRON OXIDE THIN FILMS PHOTOCATALYTIC DEGRADATION

Rajesh Kumar^{*1}, Bhajan Lal², Ajeeb Ali Mandan³, Permehri⁴, Kavita Krishna Morti⁵

^{*1,2,3}Institute of Chemistry, Shah Abdul Latif University, Khairpur, Sindh, Pakistan

⁴Dr MA KAZI Institute of Chemistry, University of Sindh, Jamshoro

⁵Liaquat University of Medical and Health Sciences, Jamshoro

¹rajeshkumar@salu.edu.pk, ²bhajan.lal@salu.edu.pk, ³ajeebalimandan@gmail.com,

⁴permehri95@gmail.com, ⁵doctor.kavita85@gmail.com

²Oric ID 0000-0002-0781-0992

DOI: <https://doi.org/10.5281/zenodo.17519287>

Keywords

Iron oxide-based thin films, Film thickness, Photocatalytic Degradation of dyes, Pyrolysis of Ferrocene and its derivatives, EDX, SEM, FTIR.

Article History

Received: 12 September 2025

Accepted: 22 October 2025

Published: 04 November 2025

Copyright @Author

Corresponding Author: *

Rajesh Kumar

Abstract

This paper examines the relationship between the thickness of the iron oxide thin layers and their photocatalytic activity in the breakdown of the organic dyes in solar radiation. Pyrolytic decomposition of organometallic precursors, including ferrocene, 4-nitrophenylferrocene and 4-ferrocenylaniline, was used on fluorine-doped tin oxide (FTO) as substrates to form iron oxide thin films. Controlled variation of precursor mass (0.1g and 0.125 g) was used to form films of varying density and morphologies. FTIR, SEM, EDX, and UV/Visible spectroscopy were used to provide structural and morphological characterization and establish the effective creation of uniform films of iron oxide where the creation of grain clusters and the surface coverage vary with the thickness of the film. The photocatalytic ability was determined by the degradation of methylene blue (MB) dye using sunlight. The rate of degradation also improved with optimal film thickness that was at its highest at more than 70 percent of the film produced using 0.125 g ferrocene (S2). To the optimal thickness, further aggregation abolished the number of active sites on the surface and hindered the flow of light, which led to low photocatalytic activity. The results prove that careful regulation of the film thickness is essential in maximizing the ratio between surfaces and volume, charge transfer mechanisms, and the general process of photocatalysis of iron oxide thin films.

Introduction

The factors that transformed materials science through nanotechnology include the ability to control matter at the atomic and molecular scale, which creates new and superior qualities that are not similar to bulk materials (Manjunatha et al., 2016; Madkour, 2019). Because of the presence of high surface/volume ratio, small grain size and

quantum confinement, nanomaterials, especially transition metal oxides, have distinctive optical, electronic and catalytic properties (Ngo and Van de Voorde, 2014).

Iron oxide is a semiconductor metal oxide with a huge amount of attention because of its abundance, chemical stability, low toxicity, and

ability to convert energy and remediate the environment (Ali et al., 2016; Dulinska-Litewka et al., 2019). The middle band gap (2.1-2.3 eV) of iron oxide enables it to absorb visible light efficiently which avails it an opportunity to be used as a promising photocatalyst in the dye degradation as well as water purification figures of speech (Sivula and Gratzel, 2013).

The growth of iron oxide as a thin film on conductive surface including fluorine-doped tin oxide (FTO) increases the speed of electricity transfer, lessens recombination losses and supplies the catalytic interface that is reusable (Barranco et al., 2016). This is because of morphology and thickness of film which profoundly influence light absorption, separation of charge, and reaction kinetics on the surface. Excessively thin films can have only enough active sites whereas excessively thick layers can prevent charge movement and photon incorporation (Goyal et al., 2010; Wang et al., 2018).

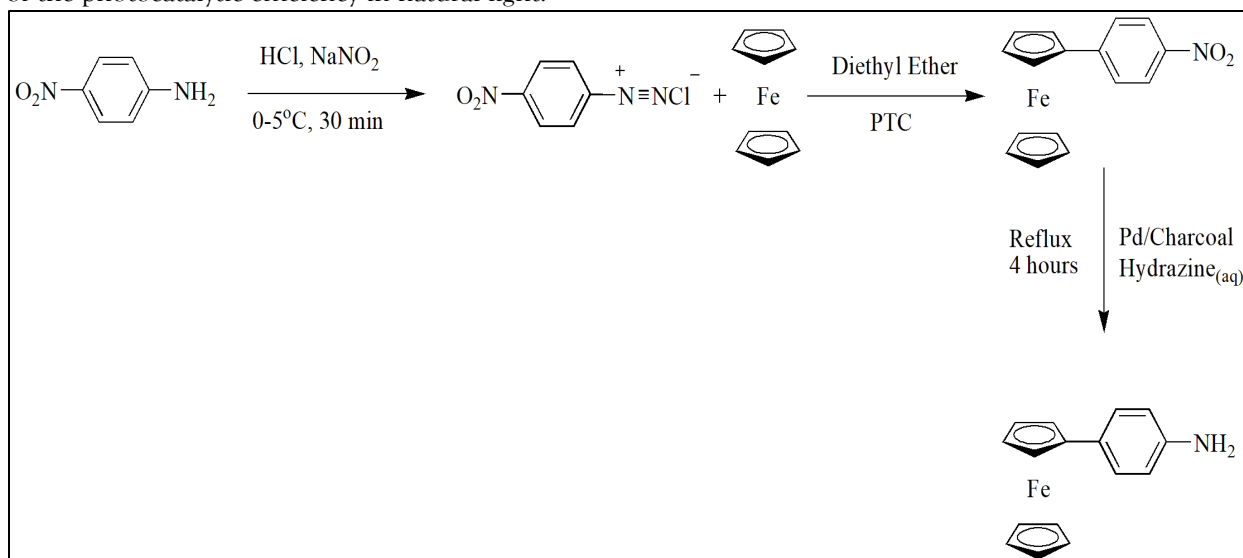
This study aims at knowing the effect of change in the thickness of the film realized through precursor loading variation on the photocatalytic performance. A route to uniform thin films is cost effective since organometallic precursors, including ferrocene and its derivatives, can be uniformly coated by pyrolysis (Campos et al., 2015). The rapid degradation of the methylene blue dye serves as the reference to the evaluation of the photocatalytic efficiency in natural light.

Materials

No further purification of analytical-grade reagents was done. These materials were ferrocene ($C_{10}H_{10}Fe$), 4-nitrophenylferrocene ($C_{16}H_{13}FeNO_2$), 4-ferrocenylaniline ($C_{17}H_{16}FeN$), the ethanol and ethylene glycol solvents. As the transducer, fluorine-doped tin oxide (FTO) coated glass (1" x 1") was chosen because of its transparency and chemical stability. Iron(III) chloride, sodium hydroxide, hydrochloric acid and ammonium hydroxide other chemicals were used in synthesizing the thin films.

Method

The reaction proceeded between 4-ferrocenylaniline and bisulfate ions to form a complex between them. The production of 4-ferrocenylaniline was done through diazonium coupling and then catalytic reduction (Ali et al., 2013). First of all, 4-nitroaniline was diazotized at 0-5 °C with sodium nitrite and hydrochloric acid. A drop of the resulting diazonium salt was added to a solution of ferrocene in diethyl ether with hexadecyltrimethylammonium bromide. The intermediate of 4-nitrophenylferrocene was isolated and purified and then it was reduced with the reaction of hydrazine hydride (80) and 10% Pd-C in ethanol to give the required amine product.

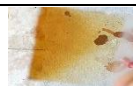







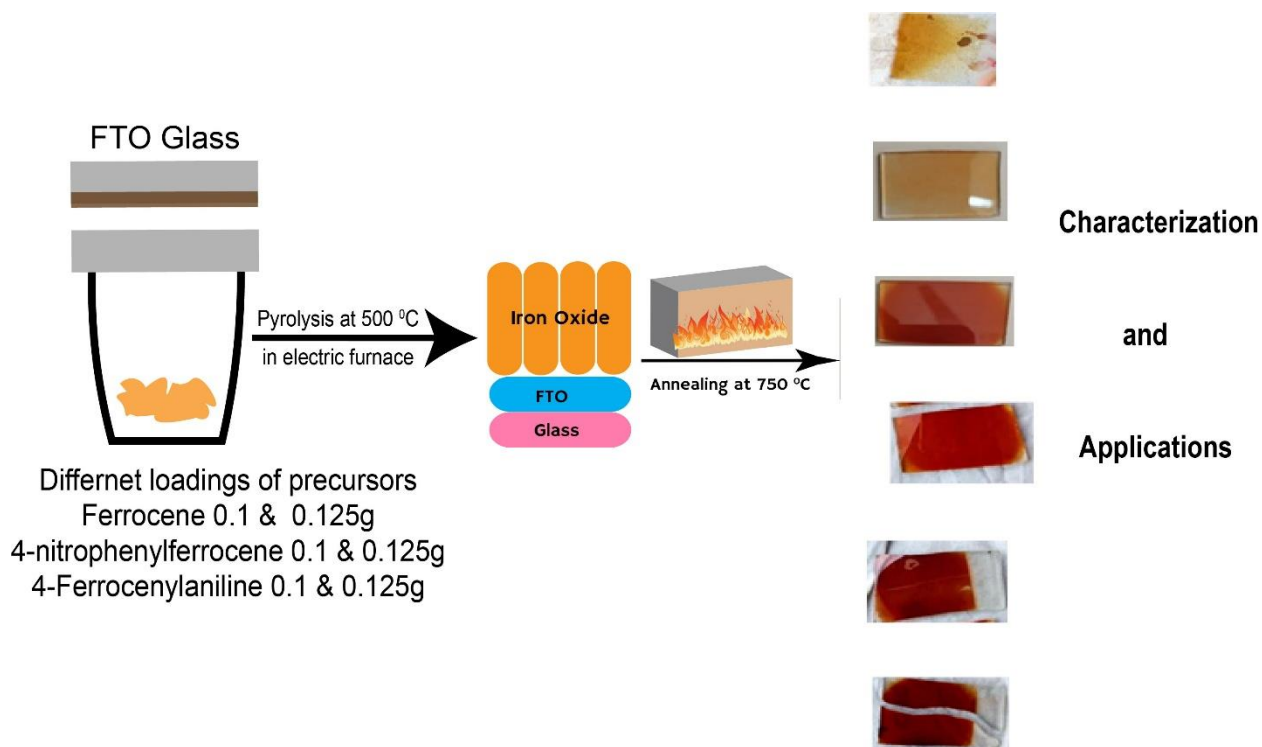
The FTO substrates were completely washed, sonicated (30 minutes) and dried (95 °C). Significant amounts (0.1g and 0.125g) of each precursor ferrocene, 4-nitrophenylferrocene and 4-ferrocenylaniline were added to a small crucible. The FTO substrate was placed facing the precursor and the crucible was heated in a pre-muffle furnace at 500 °C within 30 minutes.

Decomposition of the precursors using heat liberated iron species originating through the thermal decomposition of the precursors, which oxidized on the FTO surface to construct iron oxide thin films. Total six samples slides were synthesized from S1 to S6. The films were coded in the following way:

Work Scheme

The ferrocene was arranged from (Sigma Aldrich) while 4-nitrophenylferrocene and 4-ferrocenylaniline was synthesized in laboratory as given above. All six slides were fabricated with iron oxide thin films using different loadings as given in the table above. The precursors were subjected to pyrolysis in small crucible at or above 500 °C for 30 minutes, cooled and annealed at 750 °C for 10 minutes. FT IR, SEM, EDX, UV/Viibles, characterizations performed and finally photocatalytic abilities were compared against thickness of films.

Sample	Precursor	Precursor mass	Description	Original Slides
S1	Ferrocene	0.1 g	Thin iron oxide film	
S2	Ferrocene	0.125 g	Thicker iron oxide film	
S3	4-Nitrophenylferrocene	0.1 g	Moderate dispersion	
S4	4-Nitrophenylferrocene	0.125 g	Dense morphology	
S5	4-Ferrocenylaniline	0.1 g	Porous platelets	
S6	4-Ferrocenylaniline	0.125 g	Compact platelets	



Diffirent loadings of precursors
 Ferrocene 0.1 & 0.125g
 4-nitrophenylferrocene 0.1 & 0.125g
 4-Ferrocenylaniline 0.1 & 0.125g



Characterization

FTIR Analysis

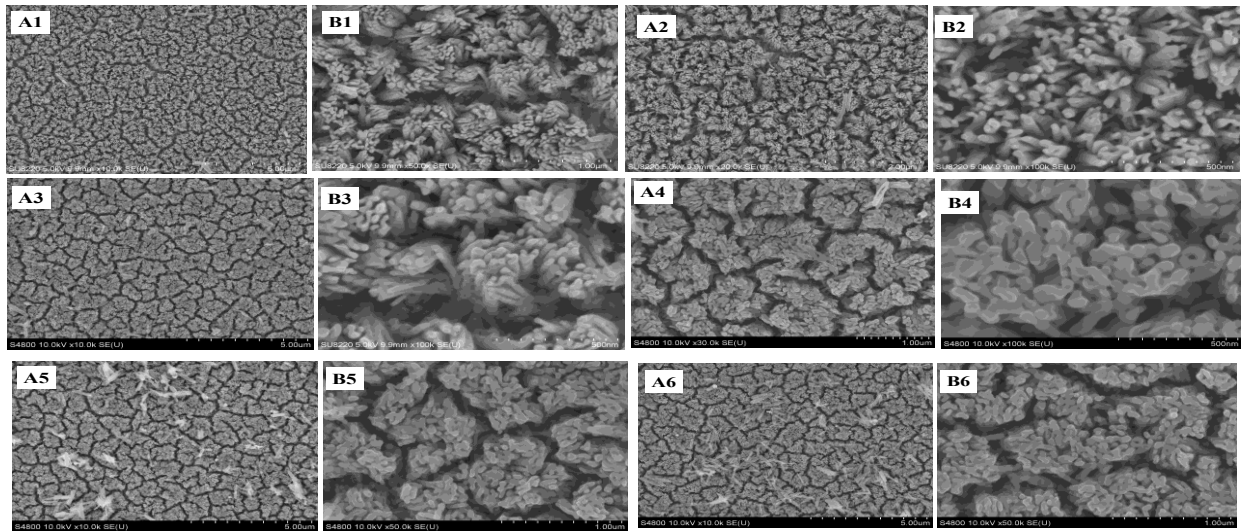
Convincing analysis of organometallic compounds to iron oxide was observed by FTIR spectroscopy (4000-400 cm⁻¹). Fe-O stretching vibration rose strongly at about 472-492 cm⁻¹. The

SEM Morphology

The scanning electron microscopy showed that there were significant variations in surface morphology as a function of film thickness. S1 (0.1 g ferrocene) had finely dispersed spherical nanoparticles that evenly covered the substrate whereas S2 (0.125 g ferrocene) had denser and

precursors had peaks attributable to -NO₂ (1549, 1323 cm⁻¹) and -NH₂ (3435, 3372 cm⁻¹) which were absent in post pyrolysis, along with the attestation of a full decomposition and oxidation of the precursors.

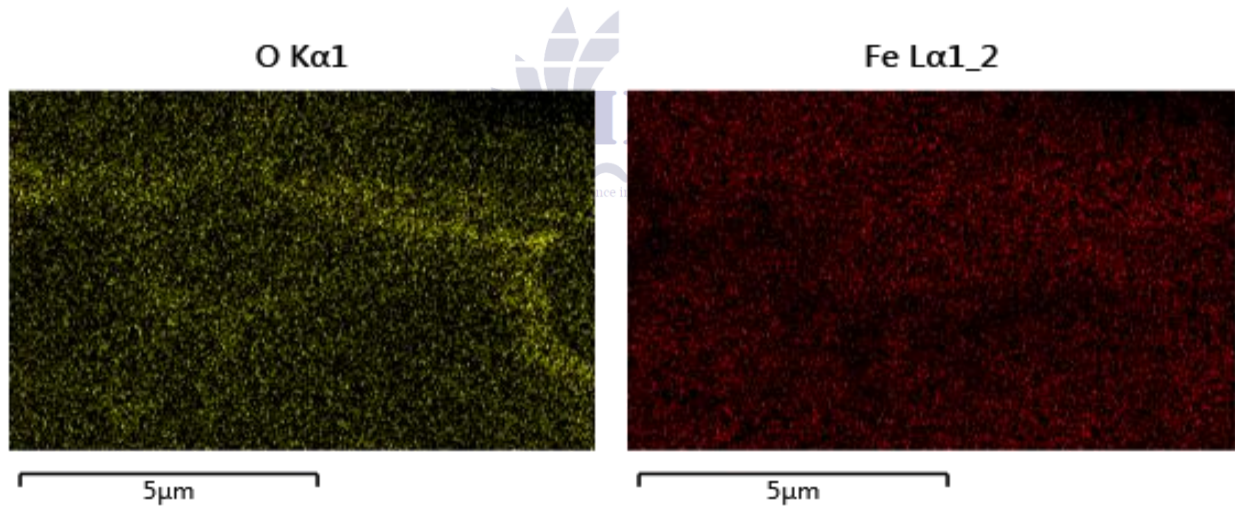
interconnected grains, which can be attributed to increased film thickness. 4-Nitrophenylferrocene based films (S3-S4) had agglomerated clusters while the 4-ferrocenylaniline films (S5-S6) formed porous platelet like structures having interconnecting holes. Two different magnifications were performed for each film.



EDX Elemental Composition

Under the EDX analysis, the elements Fe and O were found as the key elements with minor traces

of Sn present in the FTO substrate which showed that the iron oxide was formed without contamination.



Influence of morphology and Thickness.

The morphology and the thickness of the film is a key factor that dictates the photocatalytic activity. Thin films (S1, S3, S5) were good in terms of transparency and fine grain size but lower active sites. Moderate levels of thickness (S2, S6) produced better surface coverage and light absorption with excess thickness (S4) producing

agglomeration causing reduced areas of effective surface exposure.

The SEM analysis revealed that S2 had nanosized grains with compact grains that gave the best surface roughness. This texture characteristic in the nanoscale enabled an improved light capture and improved charge mobility, which resulted in less recombination between electrons and holes.

Dye Degradation Catalytic Ability.

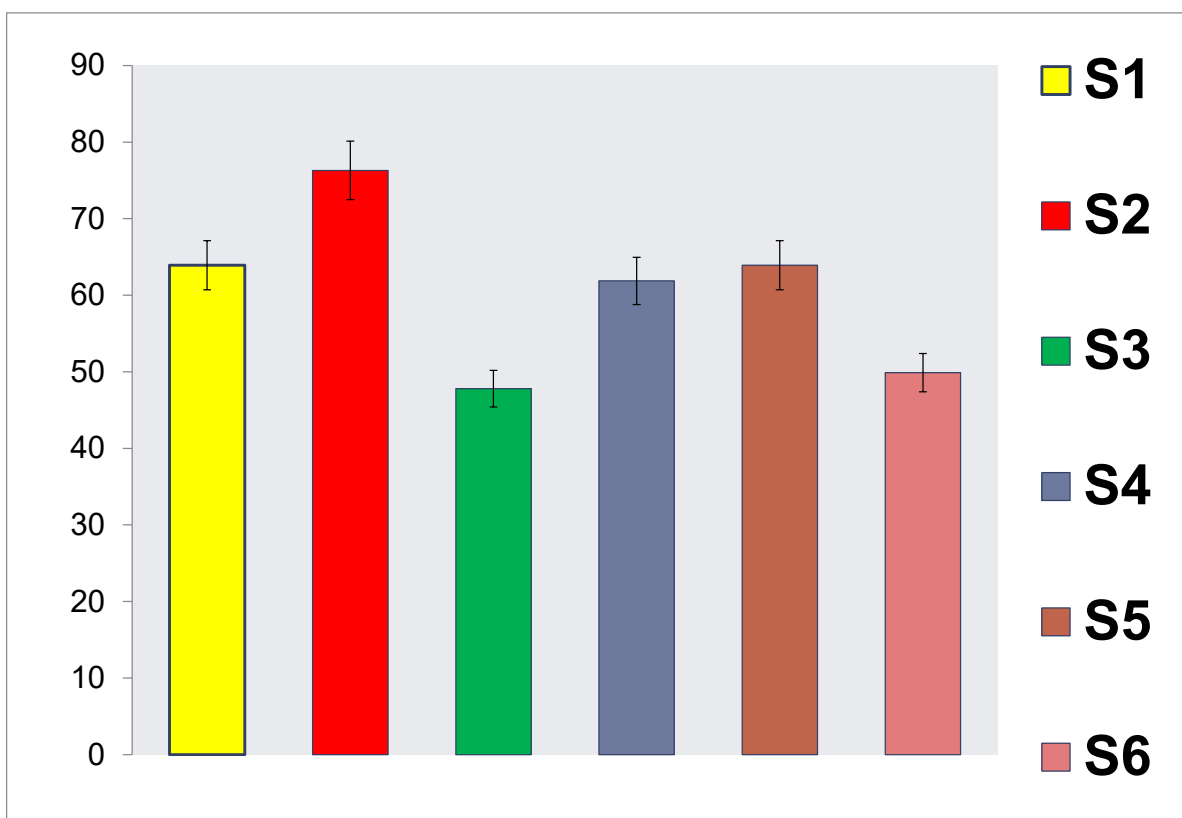
Experimental Setup

All the thin films were dipped into each of the 50 mL of 10^{-5} M solutions of methylene blue and left in the direct sunlight with constant stirring. The UV/Vis spectroscopy was used to monitor the degradation process recording the reduction in absorbance at 665 nm in 30 minutes.

S2 was found to degrade by over 70 percent in 30 minutes with optimum thickness of the film that ensured a balance between photon absorption and surface reaction kinetics. Conversely, thinner films (S1) contained few active sites whereas the thicker film S4 had a charge recombination and photon shielding.

Photocatalytic Results

MB degraded greatly in all the thin films under the sunlight. The efficiency of degradation was in order: S2 > S1 > S5 > S6 > S4 > S3



Conclusion

Thin films of iron oxide with appropriate thickness were prepared on the FTO substrate by an easy pyrolytic process. The structural and morphological studies affirmed that the homogeneous nanostructure was formed whose photocatalytic properties were heavily dependent on the thickness of the film. The best film (S2,

0.125 g ferrocene) had the maximum degradation of methylene blue almost 80% at solar irradiation, because of the increased absorption of photons, mobility of charges, and active surface area.

This paper concludes by finding out that film thickness optimization is the key to high photocatalytic efficiency. Too thick means that recombination losses will be

incurred, whereas overly thin restricts catalytic sites. Thus, an accurate control in the deposition gives a route to cost-effective, low-priced photocatalysts in environmental mitigation.

REFERENCES

- Ali, A., Zafar, H., Zia, M., ul Haq, I., Phull, A. R., Ali, J. S., & Hussain, A. (2016). Synthesis, characterization, applications, and challenges of iron oxide nanoparticles. *Nanotechnology, science and applications*, 49-67.
- Ali, S., Badshah, A., Ataf, A. A., Lal, B., & Khan, K. M. (2013). Synthesis of 3-ferrocenylaniline: DNA interaction, antibacterial, and antifungal activity. *Medicinal Chemistry Research*, 22, 3154-3159.
- Augustowski, D., Kwasnicki, P., Dziejczak, J. and Rysz, J. (2020) Magnetron sputed electron blocking layer is an effective process to enhance the activities of the dye-sensitized solar cell. *Energies*, 13(11), 2690.
- Assa, F., Jafarizadeh-Malmiri, H., Ajamein, H., Anarjan, N., Vaghari, H., Sayyar, Z., & Berenjian, A. (2016). A biotechnological perspective on the application of iron oxide nanoparticles. *Nano Research*, 9, 2203-2225.
- Barranco, A., Borrás, A., Gonzalez-Eliphe, A.R. and Palmero, A. (2016) Oblique angle of deposition of thin films perspectives. *Materials Science*, 76, pp. 59-153.
- Bhateria, R. & Singh, R. (2019) Magnetic iron oxides nanotechnological application in heavy metal removal A review. *European Water Resources Control board*. 31, 100845.
- Boholm, M. (2016). The use and meaning of nano in American English: Towards a systematic description. *Ampersand*, 3, 163-173.
- Camacho-Flores, B., Martínez-Álvarez, O., Arenas-Arrocena, M., García-Contreras, R., Argueta-Figueroa, L., De La Fuente-Hernández, J., & Acosta-Torres, L. (2015). Copper: synthesis techniques in nanoscale and powerful application as an antimicrobial agent. *Journal of Nanomaterials*, 16(1), 423-423.
- Campbell, Z. S., Bateni, F., Volk, A. A., Abdel-Latif, K., & Abolhasani, M. (2020). Microfluidic synthesis of semiconductor materials: Toward accelerated materials development in flow. *Particle & Particle Systems Characterization*, 37(12), 2000256.
- Campos, E. A., Pinto, D. V. B. S., Oliveira, J. I. S. d., Mattos, E. d. C., & Dutra, R. d. C. L. (2015). Synthesis, characterization and applications of iron oxide nanoparticles—a short review. *Journal of Aerospace Technology and Management*, 7, 267-276.
- Carenco, S., Portehault, D., Boissiere, C., Mezailles, N., & Sanchez, C. (2013). Nanoscaled metal borides and phosphides: recent developments and perspectives. *Chemical Reviews*, 113(10), 7981-8065.
- Chavali, M. S., & Nikolova, M. P. (2019). Metal oxide nanoparticles and their applications in nanotechnology. *SN applied sciences*, 1(6), 607.
- Clavero, C. (2014). Plasmon-induced hot-electron generation at nanoparticle/metal-oxide interfaces for photovoltaic and photocatalytic devices. *Nature Photonics*, 8(2), 95-103.
- Dulińska-Litewka, J., Łazarczyk, A., Hałubiec, P., Szafranski, O., Karnas, K., & Krawiec, A. (2019). Superparamagnetic iron oxide nanoparticles—Current and prospective medical applications. *Materials*, 12(4), 617.

- Falcaro, P., Ricco, R., Yazdi, A., Imaz, I., Furukawa, S., Maspocho, D., . . . Doonan, C. J. (2016). Application of metal and metal oxide nanoparticles@ MOFs. *Coordination Chemistry Reviews*, 307, 237-254.
- Ishak, N. M., Kamarudin, S., & Timmiati, S. (2019). Green synthesis of metal and metal oxide nanoparticles via plant extracts: an overview. *Materials Research Express*, 6(11), 112004.
- Khan, M., Tahir, M. N., Adil, S. F., Khan, H. U., Siddiqui, M. R. H., Al-Warthan, A. A., & Tremel, W. (2015). Graphene based metal and metal oxide nanocomposites: synthesis, properties and their applications. *Journal of Materials Chemistry A*, 3(37), 18753-18808.
- Kumar, R., Lal, B., Korai, M.B., Korai, M.A., Kumar, S. (2025) IRON OXIDE THIN FILMS ON FTO to EFFICIENT Photocatalytic Applications A Nano-enhanced Improved Approach (2025) *Annual Methodological Archive Research Review*, 3(10), pp. 11).
- Kumar, R., Lal, B., Mandan, A.A., Korai, M.B., Kumar, S. (2025) "Fabrication and Catalytic use of Iron Oxide Thin Films on FTO with Ferrocene as source of Iron), *Physical Education, Health and Social Sciences*, 3(4), pp. 1723.
- Kumar, R., Lal, B., and Mandan, AA., (2025) eco-friendly Photocatalytic Degradation of Methylene Blue Dye Using Iron Oxide Thin Film Produced by Pyrolytic Cleavage of 4-Nitrophenylferrocene, *Physical Education, Health and Social Sciences*, 3(4), pp. 2430.
- Li, Y., Zhang, W., Niu, J., & Chen, Y. (2012). Mechanism of photogenerated reactive oxygen species and correlation with the antibacterial properties of engineered metal-oxide nanoparticles. *ACS nano*, 6(6), 5164-5173.
- Madkour, L. H. (2019). *Nanoelectronic materials: fundamentals and applications* (Vol. 116): Springer.
- Maduraiveeran, G., Sasidharan, M., & Jin, W. (2019). Earth-abundant transition metal and metal oxide nanomaterials: Synthesis and electrochemical applications. *Progress in Materials Science*, 106, 100574.
- Mallakpour, S., & Madani, M. (2015). A review of current coupling agents for modification of metal oxide nanoparticles. *Progress in Organic Coatings*, 86, 194-207.
- Manjunatha, S., Biradar, D., & Aladakatti, Y. R. (2016). Nanotechnology and its applications in agriculture: A review. *J farm Sci*, 29(1), 1-13.
- Maynard, A. D. (2007). Nanotechnology: the next big thing, or much ado about nothing? *The Annals of occupational hygiene*, 51(1), 1-12.
- Nunes, D., Pimentel, A., Gonçalves, A., Pereira, S., Branquinho, R., Barquinha, P., . . . Martins, R. (2019). Metal oxide nanostructures for sensor applications. *Semiconductor Science and Technology*, 34(4), 043001.
- Sun, S.-N., Wei, C., Zhu, Z.-Z., Hou, Y.-L., Venkatraman, S. S., & Xu, Z.-C. (2014). Magnetic iron oxide nanoparticles: Synthesis and surface coating techniques for biomedical applications. *Chinese Physics B*, 23(3), 037503.
- Xu, J., Liu, J. B., Liu, B. X., Li, S. N., Wei, S. H., & Huang, B. (2018). Design of n-type transparent conducting oxides: The case of transition metal doping in In₂O₃. *Advanced Electronic Materials*, 4(3), 1700553.
- Xu, P., Zeng, G. M., Huang, D. L., Yan, M., Chen, M., Lai, C., . . . Wan, J. (2017). Fabrication of reduced glutathione functionalized iron oxide nanoparticles for magnetic removal of Pb (II) from wastewater. *Journal of the Taiwan Institute of Chemical Engineers*, 71, 165-173.

- Zhang, G., Xiao, X., Li, B., Gu, P., Xue, H., & Pang, H. (2017). Transition metal oxides with one-dimensional/one-dimensional-analogue nanostructures for advanced supercapacitors. *Journal of Materials Chemistry A*, 5(18), 8155-8186.
- Zhao, Y. S., Fu, H., Peng, A., Ma, Y., Liao, Q., & Yao, J. (2010). Construction and optoelectronic properties of organic one-dimensional nanostructures. *Accounts of chemical research*, 43(3), 409-418.

